IEEE Access
Multidisciplinary | Rapid Review | Open Access Journal

Received 11 February 2023, accepted 20 February 2023, date of publication 28 February 2023, date of current version 3 March 2023.

Digital Object Identifier 10.1109/ACCESS.2023.3250452

RESEARCH ARTICLE

An Energy-Efficient MAC Protocol for Three-Dimensional Underwater Acoustic Sensor Networks With Time Synchronization and Power Control

YE CHEN[1,2], ZHIGANG JIN[1], GUOZHEN XING[2], QINYI ZENG[2], YUEYAN CHEN[2], ZIYU ZHOU[2], AND QIULING YANG[3]

[1]School of Electrical and Information Engineering, Tianjin University, Tianjin 300072, China
[2]School of Applied Science and Technology, Hainan University, Haikou 570228, China
[3]School of Computer Science and Cyberspace Security, Hainan University, Haikou 570228, China

Corresponding author: Zhigang Jin (zgjin@tju.edu.cn)

This work was supported in part by the National Natural Science Foundation of China under Grant 52171337, in part by the Natural Science Foundation of Hainan Province under Grant RZ2100000416, and in part by the Critical Project of Hainan Province under Grant ZDYF2020199.

ABSTRACT In recent years, Underwater Acoustic Sensor Networks (UASNs) have gained considerable attention for their unique role in detecting and monitoring the underwater environment. However, due to the long propagation time, high bit error rate, and limited bandwidth of underwater acoustic systems, the design of media access control (MAC) protocols is extremely complex, especially for the power consumption of UASNs. Therefore, this paper proposes an energy-efficient MAC protocol for three-dimensional UASNs with time synchronization and power control (TDTSPC-MAC). The proposed protocol is a hybrid access scheme for three-dimensional UASN using techniques such as time synchronization, power control, clustering, layering, and sleep mechanisms. Moreover, the TDTSPC-MAC protocol uses the hierarchical concept and distributed clustering algorithm to divide the three-dimensional space, and combines time synchronization and power control strategies to avoid collisions. Besides, energy consumption is reduced through monitoring and sleep mode. Simulation results demonstrate that the proposed TDTSPC-MAC protocol has reasonable data transmission delay time, throughput, energy consumption, and other performance.

INDEX TERMS Collision avoidance, clustering, energy-efficient MAC protocol, layering, power control, three-dimensional UASNs, time synchronization.

I. INTRODUCTION

In recent years, UASNs have gained considerable attention and rapid development and have been widely used in various fields, including marine data collection, offshore exploration, disaster prevention, pollution monitoring, and tactical surveillance [1]. Underwater vehicle monitoring plays an important role in commercial and military affairs [2], [3]. However, infrared radiation remote sensing detection and non-contact space-borne microwave technology can achieve large-scale and rapid detection for the monitoring of underwater vehicles [4]. Unlike terrestrial wireless sensor networks, sound waves travel better underwater than electromagnetic waves and light [5]. However, the low propagation speed of sound waves will cause high latency because the sound velocity of underwater acoustic communication is about 1500m/s, five orders of magnitude lower than radio signals [6]. Moreover, the available bandwidth of the underwater channel is usually less than 15kHz, and the transmitted information is limited [7], causing significant difficulties for underwater acoustic communication. Besides, UASN needs to cover a large area of the ocean, which leads to the sparseness of node deployment. Furthermore, most nodes are powered by batteries with limited energy, making it difficult

The associate editor coordinating the review of this manuscript and approving it for publication was Mauro Fadda.

to supply energy [8]. Therefore, the design of the MAC protocol must be based on energy saving to effectively control power consumption.

The performance of any protocol depends only on the application and design requirements. The existing protocols are highly selective. Since the design core of an ideal UASN is energy efficiency and reliability, communication efficiency and consumption can evaluate the design of these MAC protocols [9]. Although the energy consumption of ordinary sensor nodes is low, the low capacity and high propagation delay of underwater acoustic sensors will lead to a serious decline in the communication performance and efficiency of UASNs. Moreover, the energy waste of the MAC layer is mainly caused by packet collisions, idle snooping, crosstalk, and control packet overhead [10]. Therefore, the MAC protocol design in this paper focuses on energy efficiency and reliability.

Compared with terrestrial networks, UASNs have important depth information, making them three-dimensional networks. A difficult problem in UASNs is to deploy minimum sensor nodes, ensuring that all nodes in the network are within the sensing scope of at least one sensor and that all sensor nodes can communicate with each other through multi-hop paths. To solve this problem, Karim et al. [11] proposed an anchor nodes-assisted cluster-based routing protocol for reliable data transfer. Under the sphere-based communication and sensing model, the node was placed at the center of each created virtual cell based on the truncated octahedral mosaic. This solution provides ideas for researching the MAC protocol of three-dimensional underwater space.

In this paper, an energy-efficient MAC protocol is designed for three-dimensional UASNs. The main contributions of this paper are summarized as follows: Firstly, after analyzing the energy consumption of each sensor node, an energy-efficient scheme is designed according to the transceiver state and standby state of each sensor node. Emphatically, the invalid transceiver caused by communication collisions can be avoided through clustering, layering, time synchronization, and power control methods. Secondly, a three-dimensional network topology is constructed to avoid communication collisions between sensor nodes and effectively monitor a specified underwater area.

The remainder of this article is organized as follows: Section II describes the work related to the UASN MAC protocol. Section III describes the structure of a UASN. Section IV describes the TDTSPC-MAC protocol. Section V presents a collision-avoidance design of three-dimensional space. In Section VI, the proposed MAC protocol is verified through simulations, and the experimental results are analyzed. Finally, Section VII summarizes the article and suggests future work.

II. RELATED WORK

Various factors such as application requirements, marine environment characteristics, underwater acoustic communication characteristics, and sensor resource constraints significantly impact the design and development of three-dimensional network architecture and protocol stack. Therefore, numerous studies have been conducted on UASNs, considering the unique challenges of the underwater environment, including deployment, spatial-temporal uncertainty, time synchronization, multi-path propagation, and energy consumption [12], [13], [14], [15], [16].

Zhang et al. developed an analytical model to quantify network performance for sensor packet queuing delays and packet error probabilities [17]. The model determined the minimum data aggregation density required to meet the requirements of the underwater sensor density for packet error probability in calculating packet queuing delay. Chen et al. proposed a new cross-layer protocol stack for three-dimensional UASNs and developed a cross-layer design combined stack [18]. This protocol can be used for long-term ocean monitoring, achieving energy efficiency, and improving network performance. Dhongdi et al. proposed a network protocol that included TDMA MAC, dynamic routing stacks, and network protocol stacks for services such as time synchronization, cluster head rotation, and power level management [19]. Moreover, Pompili et al. proposed deployment strategies for two-dimensional and three-dimensional communication architectures for UASNs [20]. In both deployment architectures, the minimum number of sensors for a given target water body was determined through mathematical analysis to achieve the best sensing and communication coverage. Furthermore, the robustness for node failure was studied, and the number of possible redundant sensor nodes was provided.

Topology control in the three-dimensional UASN is of great significance to ensure the reliable and efficient operation of the network. Generally, the network topology of the underwater MAC protocol includes the centralized (*e.g.*, star or tree) and cluster topology. Zhang et al. proposed a topological control strategy based on Complex Network Theory and constructed a dual cluster structure with two types of cluster heads to ensure connectivity and coverage [21]. Liu et al. used the cube as the base unit, divided the monitoring area into a three-dimensional basic cluster structure, and arranged rotating temporary control nodes in the cluster to ensure maximum sensor coverage and active node connection rates for the entire network [22].

In 2019, Alfouzan et al. proposed a layered deployment of sensor nodes for collisions caused by high latency [23]. In the same year, Alfouzan et al. proposed an asynchronous positioning scheme in which the nodes were randomly distributed across four layers, and the beacons were mobile [24]. Moreover, Ahmed and Cho proposed an underwater layering protocol that used collaborative communication instead of standard multi-hop transmission and added a relay cooperation model during the data transmission phase, ensuring the link quality of underwater channels [25]. Morozs et al. proposed a hierarchical network architecture consisting of an underwater fixed sensor network layer and the autonomous underwater vehicle (AUV) information acquisition layer [26].

This information acquisition system does not require modification or initialization of the underlying fixed sensor network, which makes it flexible and deployable.

Generally, a typical UASN contains hundreds or more randomly deployed sensor nodes. However, the UASN will undergo dynamic topological changes due to the long delay time of acoustic signal propagation and the node migration caused by water flow. Therefore, improper handling may lead to transmission errors, missing links, collisions, and congestion. To solve these problems, Xing et al. proposed a clustering method based on game theory and Nash equilibrium [27]. Anupama et al. proposed a clustering algorithm based on sensor nodes' three-dimensional hierarchical network architecture [28].

Collisions in the propagation process are possible due to the spatial-temporal uncertainty of underwater communication. Hence, time synchronization is a key foundational technology for any distributed system underwater. In UASNs, global positioning system (GPS) signals are unavailable, and synchronization systems are mainly based on acoustic communications [29]. Jin et al. proposed an ordered scheduling MAC protocol based on a handshake mechanism for transmitting packets related to computed lists [30]. Moreover, Li et al. proposed a full-duplex collision avoidance (FDCA) MAC protocol based on a handshake mechanism that avoided collisions by passively obtaining positioning information (propagation delays of neighboring nodes and regular transmission schedules) [31]. Liu et al. proposed a high-latency time synchronization algorithm considering the slow speed of undercarriage acoustic wave transmission [32]. Furthermore, Wang et al. proposed a cluster-based terminal services algorithm in which cluster head nodes and nodes in the cluster achieved time synchronization using interactive patterns for sending and receiving messages [33]. Gong et al. also proposed a robot-assisted underwater sensing network algorithm that combined positioning and time synchronization [34]. An underwater robot was used as a moving anchor, and positioning and time synchronization were performed with the help of GPS.

The majority of the proposed MAC protocols are concerned with energy consumption in UASNs. Kim et al. designed energy-efficient MAC protocols using monitoring and wake-up methods [35]. Under the condition of adjustable transmission power, Wang et al. proposed an underwater power control protocol that utilized dynamic transmission power regulation and a new rate adaptation algorithm to improve the efficiency of spatial multiplexing [36]. Moreover, Lmai et al. proposed a MAC protocol that used lower transmission power to send packets and periodically added notification signals with maximum power during packet transmission to avoid collisions [37].

An efficient method to improve the network throughput is reusing spatial resources. Su et al. combined the hardware design of underwater orthogonal frequency division multiplexing (OFDM) modems to develop an adaptive rate algorithm based on the signal-to-interference-plus-noise ratio (SINR) to improve the efficiency of spatial multiplexing [38]. Zhou et al. proposed an adaptive power-efficient time synchronization scheme (APE-Sync) for mobile UASNs that adjusted the transmit power and combined the Doppler-Enhanced synchronization protocol and the Kalman filter tracking the clock skew to reduce energy consumption [39]. Su et al. proposed a joint power control and rate adaptation MAC protocol for UASNs [40]. Qian et al. proposed a MACA-based power control MAC protocol (MACA-PC) that dynamically adjusted different power levels for RTS-CTS and DATA, reducing the energy consumption of data transmission and prolonging the life of the nodes [41]. Guo et al. introduced an adaptive propagation-delay-tolerant collision-avoidance protocol (APCAP) for the MAC sub-layer of UASN. The APCAP improved the efficiency and throughput with a large propagation delay [42]. To ensure transmission fairness, Hossain et al. proposed a spatially equitable multi-access control protocol that could be cleared by delay Send frames to avoid collisions [43].

Therefore, this paper proposes an energy-efficient MAC protocol for UASNs, considering the need to deploy in a three-dimensional underwater space. The proposed protocol adopts the concepts of stratification and clustering, combined with time synchronization and power control, to plan underwater time and space to avoid network communication collisions, which can save energy consumption and extend the life of the UASN.

III. PROBLEM DESCRIPTION AND SYSTEM MODEL

A. PROBLEM DESCRIPTION

The energy consumption model of an underwater acoustic sensor network is quite different from that of a terrestrial wireless sensor network due to the characteristics of the underwater acoustic channel. The energy model of the sensor is as follows [44]:

The energy consumed for data transmission is defined as:

$$E_t(n, d) = n \times E_{tr} + n \times E_e \tag{1}$$

where E_t is the energy consumed in transmission, E_{tr} is the energy consumed by the electronics for transmitting and receiving 1-bit data measured in (j/b), n is the number of bits, and E_e is defined as:

$$E_e = E_0 \times d^k \times \varphi^d \tag{2}$$

where d is the distance between the transmitter and receiver, k is the spreading factor (for spherical spreading $=$ 2 and or cylindrical spreading $=$ 1) with value $k = 1.5$, E_0 is the power threshold that the data can be received by the node and φ is a frequency-related term obtained from the absorption coefficient, which is defined as:

$$\varphi = 10^{\frac{A(f)}{10}} \tag{3}$$

where $A(f)$ is in dB/km and frequency in kHz. Where f is the absorption coefficient, and it is the function of the frequency.

$A(f)$ can be calculated from Thorp's expression [45] for the frequencies above a few hundred Hz as:

$$A(f) = \frac{44f^2}{4100+f^2} + \frac{0.11\,f^2}{1+f^2} + \frac{0.275\,f^2}{10^3} + \frac{3}{1000} \quad (4)$$

Then, the energy consumed by a sensor node to receive n bits of data is:

$$E_r(n) = n \times E_{tr} \quad (5)$$

The energy consumed by a sensor node for idle listening is expressed as:

$$E_I(n) = n \times E_{tr} \times \eta \quad (6)$$

where η is the ratio of reception and idle listening energy.

Then, the energy consumption of the underwater acoustic sensing node during communication is analyzed [46]. Figure 1 shows the power consumption of the sensor of a UASN. It can be seen that the energy consumed by the underwater acoustic signal's transmission and reception accounts for about 60% of the node's total energy consumption. Therefore, the key issues of energy-saving MAC protocols will be avoiding communication collisions, improving communication efficiency, and reducing the energy consumption of UASNs. Besides, time-sharing monitoring is possible since the underwater environment does not change significantly in a short period, and nodes can be woken up autonomously. In contrast, the UASN's sleep mode consumes much less energy than the idle mode. Thus, the energy consumption of UASN can be significantly reduced, and its life can be extended by making it sleep during idle time and wake up when needed.

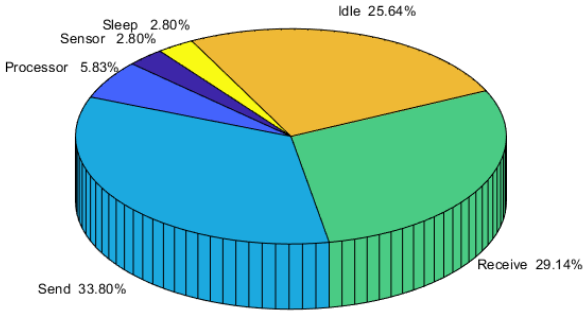

FIGURE 1. Power consumption of a sensor of UASN.

1) COLLISION ANALYSIS FOR THE SYSTEM

a: SPATIAL-TEMPORAL UNCERTAINTY PROBLEM

The high delay in underwater acoustic propagation causes the spatial-temporal uncertainty of UASN communication. The spatial-temporal uncertainty affects reception time, transmission time, and propagation delay to the destination [47]. Spatial-temporal uncertainty refers to determining the state of a channel by considering the location of the receiving node and the transmission time of the transmitting node. First, the collision of the destination node (that is, two packets arriving at the receiving node at the same time) depends on the transmission time and propagation delay of the sending node. Second, the distance between the nodes creates uncertainty about the current channel state, and collisions can occur even if other nodes in the cluster communicate separately.

Generally, high propagation delays may lead to underwater communication collisions. Figure 2 shows two examples of spatial-temporal uncertainty. Specifically, nodes A and C can send packets simultaneously, as shown in Figure 2 (a). When the propagation delays of the two senders are different, the receiving time of the two packets is sorted. Figure 2 (b) shows that when nodes A and C transmit packets at different transmission times, node B will collide.

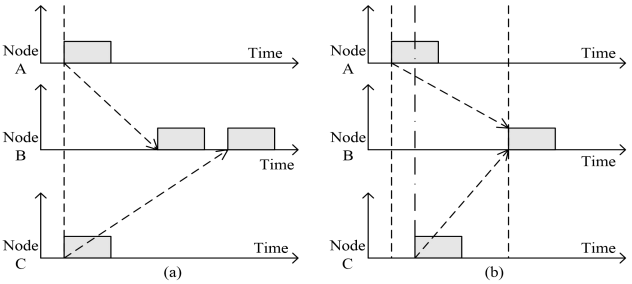

FIGURE 2. Spatial-temporal uncertainty problem: (a) No collisions when sending at the same time; (b) Collisions when sending at different times.

b: HIDDEN TERMINAL PROBLEM

A hidden terminal problem can be defined as a sensor node whose other sensor is unknown. The terminal hiding may cause a collision when a sensor node cannot detect that another node is interfering with its transmission [48]. Moreover, collisions may occur when two sensors transmit data to the same target sensor. Figure 3 illustrates the hidden and exposed node problems. Specifically, sensors A and C cannot perceive each other when both are visible to sensor B. Therefore, sending packets from sensors A and C may lead to collisions with sensor B. Furthermore, the hidden terminal problem may lead to low throughput and high energy consumption. These issues should be properly resolved to avoid any collision between sending and receiving schedules.

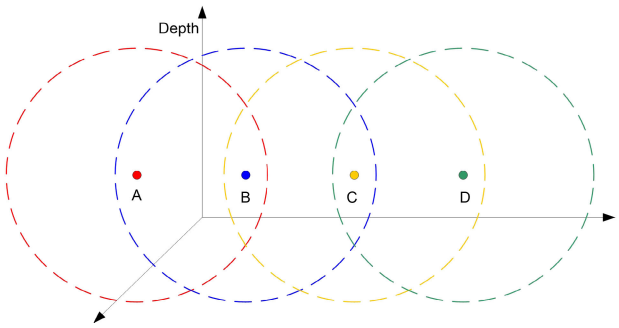

FIGURE 3. Hidden and exposed node problems.

c: EXPOSED TERMINAL PROBLEM

The node exposure problem may occur when a sensor node delays transmission due to receiving another signal [49]. Specifically, sensors A and D in Figure 3 are single-hop neighbors of sensors B and C, respectively. Sensors A and D can receive packets sent by sensors B and C without collision, respectively. However, sensors B and C are blocked from sending packets because both sensors are within the transmission range of each other, even if the receiving sensors A and D are out of their respective transmission ranges.

Furthermore, if sensor A communicates with sensor B, sensor C will not be able to send packets to sensor D after the channel is detected. Sensor B may interfere with its one-hop neighbor, sensor C, but sensor D could have received the data packet sent by sensor C.

2) LISTENING AND HIBERNATION MODELS OF THE SYSTEM

Typically, the nodes are powered by batteries, meaning they have a limited source of energy [50]. Hence, it is difficult to charge or replace batteries for underwater sensor nodes from the perspective of cost and technology at this stage. Therefore, the working time of UASNs must be extended by reducing the energy consumption of the nodes and improving efficiency.

The design of the MAC protocol should pay extra attention to energy efficiency, considering the application of UASNs. Normally, the energy consumption depends on the distance of acoustic signal transmission. The relationship between transmission power and distance follows the quadratic function [51]. Hence, the high data volumes are incompatible with long distances from a power consumption perspective. Therefore, balancing energy consumption and communication is a key issue.

As shown in Figure 1, there are four main parts of the wasted energy consumption of a sensor node in UASN. The first part is the collision. The current packet must be dropped and re-transmitted to another node when a collision corrupts a packet, thus increasing energy consumption and delay. The second part is excessive listening, meaning one node receives messages that others should receive. The third part is idle listening, which prevents packet errors and leaks when the node monitors the idle channel. The fourth part is that the receiving node is not ready to receive the packets sent by the sender, and the packets must be re-sent again, resulting in energy loss.

Considering the above problems, an energy-efficient MAC protocol based on collision-free design and sleep mode is proposed to reduce the energy consumption of UASNs.

B. SYSTEM MODEL

A three-dimensional UASN is designed to monitor a certain area of the sea. There are three types of sensors. One is that node located on the water surface is called the buoy node, and it is set at a predetermined position to collect and forward data. Another kind of special node is called the relay node, which forwards data packets between the buoy node and the ordinary node, and is also the cluster head of the network cluster, also known as the cluster head node. The last one is the ordinary node that perceives the characteristics of the submersible. Figure 4 shows the architecture of the three-dimensional UASN. The surface buoy node is used to achieve GPS positioning with the satellite through wireless signals, and the time synchronization with the underwater sensor node is realized [52]. The underwater node transmits information to the surface buoy through acoustic signals. Then, the buoy transmits information to the onshore control center through satellite or surface communication ships using radio signals. The ordinary nodes are randomly distributed in the three-dimensional underwater space of different depths and regions to monitor large submersibles in the sea, and the data are forwarded to the buoy node through relay nodes (cluster heads).

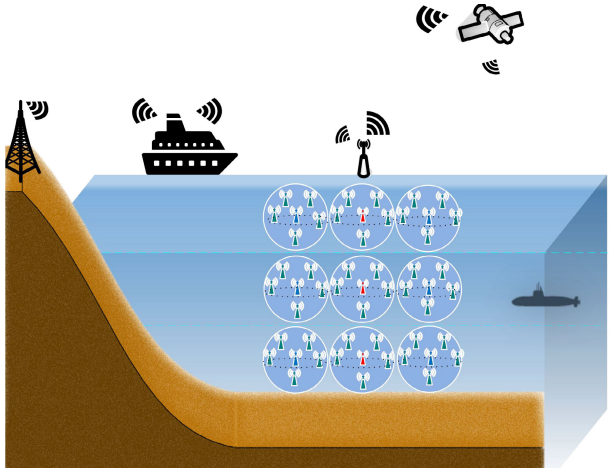

FIGURE 4. Architecture of the three-dimensional UASN.

The network topology considered in this article is shown in Figure 5. The relay and buoy nodes are deployed in different locations in three-dimensional space, divided into different layers (A, B, C) according to depth. All layers work together to monitor local ocean space. Moreover, each layer can be divided into different cell spaces, and the relay nodes in the center of each unit space and the ordinary nodes in the unit space are clustered. Afterward, the relay node of the unit transmits the collected information to the central node of each layer after collecting the information in the cluster. Then, the central node of each layer transmits the information to the buoy node on the surface. It is assumed that the cluster head node and buoy can move slightly in the horizontal direction, considering the mobility of ocean currents, and their vertical movements can be neglected.

In the UASN, the three horizontal layers have different time slots. Besides, two adjacent cell spaces in each layer work in different time slots. In this case, the same type of cell space in the same layer can operate within the same time slot. Hence, vertical collisions in different horizontal layers can be avoided with time synchronization and power control.

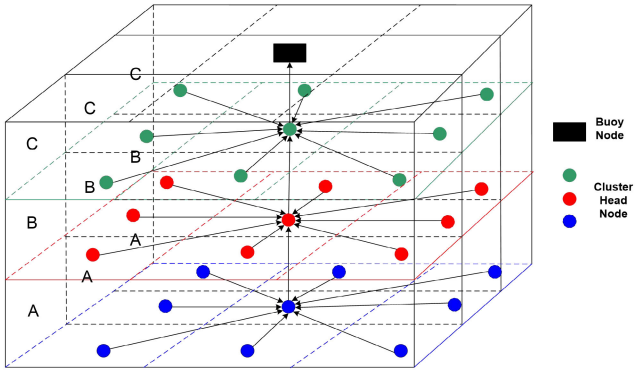

FIGURE 5. Network topology considered in the proposed framework.

Moreover, the nodes' clustering method and power control scheme can eliminate the horizontal collisions between different cell spaces in each layer.

Figure 6 shows the timeline of the proposed TDTSPC-MAC protocol, which consists of four operational phases: the update, scheduling, operational, and dormancy phases. It is worth noting that the protocol sets the start time of each stage so that all sensors start and end together and can run a certain phase individually.

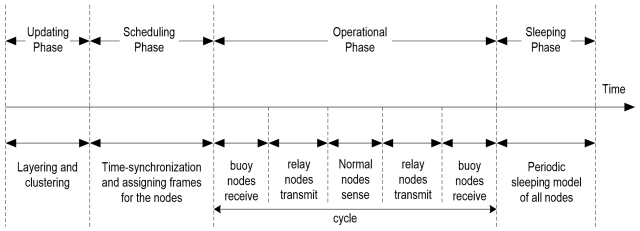

FIGURE 6. Timeline of the proposed TDTSPC-MAC protocol.

First, the adjacent single-hop nodes are identified and clustered by exchanging update messages in the update phase. The second phase is time synchronization. The time slots are allocated for each node and cell space. The third phase is the operational phase, in which the sensor network transmits the information to the buoy node and then to the ground station through electromagnetic waves. Finally, the fourth phase is the sleep phase. All nodes are in listening and sleeping modes to save energy.

IV. TDTSPC-MAC: AN ENERGY-EFFICIENT MAC PROTOCOL

A. HIERARCHICAL DESIGN OF THE UASN

Firstly, the coverage area of the sensor network is divided into three different types of horizontal layers named the A, B, and C layers. The width l of each layer equals the transmission range R_{th} used by the cluster head node for inter-cluster communication. The layers can be determined by (Z_{area}/l), where Z_{area} is the coverage depth of the sensor network [53]. This specification can prevent transmission overlap between adjacent layer nodes.

As mentioned above, the UASN contains buoy, relay, and ordinary nodes. Next, the nodes need to be divided into layers, while the relay nodes are evenly distributed in the underwater space and anchored in a fixed position (the center of each cell space). It is assumed that the ordinary nodes are randomly distributed in the sea to be monitored, drifting with ocean currents, and each node has a buoyancy device that can change its depth. Hence, the density of nodes covering local areas can be adjusted. Moreover, each sensor node can use the internal pressure gauge to determine its depth. The depth information can be used to determine which layer the node belongs to:

$$S_{lay} = \frac{d_{depth}}{l} mod M_n \tag{7}$$

where d_{depth} is the depth information of the nodes, and M_n is the total number of layer types (layers A, B, and C) [54].

Since each node knows its layer, ordinary nodes can communicate with cluster head nodes in the same layer. In the update phase, the cluster head node will broadcast information within the set range and then form a cluster with ordinary nodes within the single-hop range.

Each type of layer is assigned a unique time slot. To prevent a collision, the adjacent cell space clusters in the same layer operate in different frames (times), and the nodes in the clusters also allocate different time slots. Moreover, the ordinary nodes in different layers can adjust the signal power to be in a cluster of the same layer. The relay nodes can adjust the signal power to complete intra- and inter-cluster communication. Similarly, different time slots can facilitate communication between ordinary and cluster head nodes, relay and relay nodes, and relay and buoy nodes.

B. CLUSTER DESIGN OF THE UASN

The clustering is formed by cluster heads and ordinary nodes within their communication range in three-dimensional space, and ordinary nodes transmit information to cluster head nodes through interaction [55]. It is assumed that the cluster head nodes are evenly distributed in the center of each unit space, and each node can determine its layer using depth information. Therefore, nodes of different layers cannot form a cluster. There will be no clustering problem in the same layer if the ordinary node only receives the invitation information of a cluster head node. However, when an ordinary node is located in the overlapping communication range of two adjacent cluster head nodes, it would be difficult to decide which cluster head node to cluster. Figure 7 illustrates the partition of spatial cluster nodes. The ordinary nodes C and D receive cluster invitations from cluster head nodes A and B, respectively.

To solve this problem, the ranging method is used to measure the distances d_{AD} and d_{BD} between the ordinary node and the cluster head nodes. It can be seen from Figure 7 that node D is in the cell space where cluster head node B is located in the middle. The three points form a triangle plane ABD. Since the distance (d_{BD}) between B and D is less than the

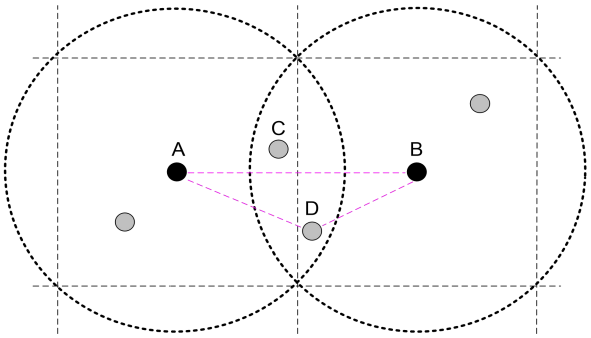

FIGURE 7. Partition of spatial cluster nodes.

distance (d_{AD}) between A and D, node D will be clustered with cluster head node B. Thus, the ordinary nodes can judge their cluster head nodes by ranging and then cluster with the nearest cluster head node.

Time of arrival (ToA) is the simplest and most intuitive distance estimation technique. It estimates the distance between nodes by measuring the propagation time of the signal, requiring precise synchronization between the two nodes. In this case, the distance between two nodes is proportional to the time required for the signal to propagate from one node to the other. Moreover, the time when the signal leaves the node must be in the transmitted packet. Thus, if node A sends a signal at the moment t_1 and reaches the receiving node D at the moment t_2, the distance between the two nodes is:

$$d = V_s \times (t_2 - t_1) \tag{8}$$

where V_s is the propagation speed of the acoustic signal, which is 1500 m/s.

C. TIME SYNCHRONIZATION DESIGN OF THE UASN

Even if the clocks of the two nodes are fully synchronized at the beginning, there will be inconsistencies due to changes in the surrounding environment. For example, their clocks may drift when the nodes experience temperature, pressure, and battery voltage changes [56]. This change accumulates over time, making nodes work at different times. Since the proposed TDTSPC-MAC protocol relies on the unified planning of network time, the network time needs to be synchronized.

The time synchronization of nodes includes time synchronization between buoy and relay nodes, between cluster head nodes, and between cluster heads and ordinary nodes in each cluster. These three processes are similar. Taking the time synchronization process of the cluster head and ordinary nodes in the cluster as an example. The standard reference time is transmitted to other nodes through the cluster head node to realize time synchronization, as shown in Figure 8.

Specifically, a quantization mechanism is adopted that allows the differences in propagation delay between different packets and uses continuous network communication to achieve time synchronization of each node.

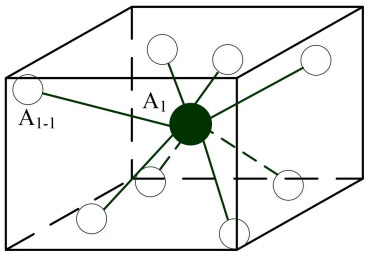

FIGURE 8. Synchronization for nodes.

1) QUANTITATIVE REPRESENTATION OF NODE MOTION

In the quantization step, the positions of ordinary nodes and cluster head nodes are quantified so that multiple ToA measurements from bidirectional communication are associated with the same pair of quantitative positions [57]. Specifically, two packets $i, j\ (i \in N^a, j \in N^b)$ are considered. If $l_i = l_j = l$, the two sets of ordinary node locations (g_i, g_j) and cluster head node locations (P_i, P_j) have the same quantization positions K_ρ and $U_{l,v}$, respectively. Assuming that $T_i^{pd} = T_j^{pd}$, and variables v and ρ can be enumerated for position quantization.

To quantify the position of the cluster head node, subset $i, j \in N$ is introduced that includes all packets associated with the same anchor node l so that there is a fixed threshold for each pair $i, j \in U_{l,v}$, $\|P_i - P_j\| < \triangle$ of packets $\triangle$. Next, the position P_i, $i \in U_{l,v}$ is associated with the quantified position $U_{l,v}$. Similarly, a subset of packets $R_\rho \in N$ is formed, and each pair of packets $i, j \in R_\rho$, $d_{i,j} < \triangle$ is made to quantize the position of the ordinary node, and the position j_i, $i \in R_\rho$ is associated with the quantified position K_ρ. It is possible to associate a single packet with multiple subsets $U_{l,v}$ and R_ρ.

2) ESTIMATION OF CLOCK SKEW AND OFFSET

Next, the quantization position is used to estimate the clock skew S_l and offset Y_l. For the data sets $l = 1, \ldots L$, the subsets are separately defined as $N_l^a \subseteq N^a$ and $N_l^b \subseteq N^b$, along with their cardinalities N_l^a and N_l^b, respectively. The subsets include all data packets l related to the cluster head node. Considering a pair of packets $i, j\ (i \in N_l^a, j \in N_l^b)$, the positions (P_i, P_j) and (m_i, m_j) are mapped to the same quantization positions $U_{l,v}$ and K_ρ, respectively. Assuming that the result M_l of this mapping increases for each cluster head node with the increase in the quantization threshold. As mentioned above, the difference between the propagation delay in T_i^{pd} and T_j^{pd} is ignored, thus obtaining an equation M_l as:

$$\frac{R_i + T_j}{S_l} - \frac{2Y_l}{S_l} = R_j + T_i + \gamma_i + \gamma_j, i \in N_l^a, j \in N_l^b \tag{9}$$

Introducing the variable vector $E_l = [E_l(1), E_l(2)]^T = \left[\frac{1}{S_l} + \frac{Y_l}{S_l}\right]^T$, Eq. (9) is expressed as a linear matrix equation:

$$B_l E_l = b_l + \theta_l \tag{10}$$

where B_l is the matrix $[M_l \times 2]$, $\left[R_i + T_j, -2\right]$, b_l and θ_l are the column vectors of appropriate length, and the elements

are $R_j + T_i$ and $\gamma_i + \gamma_j$, $i \in N_l^a, j \in N_l^b$. Next, the least squares estimation is applied:

$$\widehat{E}_l = \left(B_l^T B_l\right)^{-1} B_l^T b_l \tag{11}$$

The covariance matrix $\widehat{E}_l$ is:

$$Q_E = 2\sigma^2 \left(B_l^T B_l\right)^{-1} \tag{12}$$

The main diagonal elements of the covariance matrix are proportional to $\frac{1}{M_l}$ and $\frac{1}{M_l{}^2}$. Therefore, for larger M_l, the variance of the estimated $\widehat{E}_l(1)$ and $\widehat{E}_l(2)$ is expected to be much smaller than σ^2.

3) ESTIMATED PROPAGATION DELAY

For packets $i \in N_l^a, j \in N_l^b$, the estimated propagation delay of the ordinary node is:

$$\widehat{T_i^{pd}} = R_i \widehat{E}_l(1) - \widehat{E}_l(2) - T_i, i \in N_l^a \tag{13}$$

$$\widehat{T_j^{pd}} = \widehat{E}_l(2) - T_j \widehat{E}_l(1) + R_j, j \in N_l^b \tag{14}$$

The propagation error is a function of ToA measurement error, clock tilt, and offset estimation error.

D. POWER CONTROL OF TDTSPC-MAC PROTOCOL

The proposed design aims to minimize energy consumption and provide reliable connections between network nodes. Therefore, the large-scale system and channel parameters that determine the network energy consumption are analyzed to evaluate the trade-off in the proposed design.

Assuming that the selected multi-access strategy can support any number of connections, the energy consumption is identified as a function of the network topology, that is, as a function of the connections established between network nodes [58]. Although the geometry of the network is known, the location of ordinary nodes cannot be accurately determined. Besides, it is assumed that the nodes are evenly distributed to provide optimal coverage.

To quantify the energy consumption of the network, a simplified scenario is studied in which a controller node and N nodes are linearly arranged along a length of r. Since the nodes are evenly distributed, the distance between each neighboring node (including the distance from the base station to the nearest node) is r/N. In this case, the communication policy is that each node transmits information only to its nearest neighbor nodes (multi-hop point-to-point topology).

Next, it is necessary to determine the energy required to transmit a single packet of T_P. Assuming that N relays have passed from the main node to the node with a distance of r, and the received power level is P_0, the transmitter's power must be x^k, then the received power level of the signal will meet the requirements of transmission distance x. Therefore, the attenuation value $W(x)$ is expressed as:

$$W(x) = x^k \varphi^k \tag{15}$$

Each node needs to transmit within the duration T_P and at the power level $P_1 = P_0 W(r/N)$. The duration T_P is the time in which a data packet can be transmitted from one node to another over a distance of r/N. Therefore, the total energy transmitted by N-hop flowers is expressed as:

$$E = NP_1 T_P = NP_0 W(r/N) T_P \tag{16}$$

Each node has a packet to transmit, and the total energy consumed by packet trunking is defined as:

$$\begin{aligned} E_{rel} &= P_0 T_P W(r/N) + P_0 2\, T_P W(r/N) + \ldots \\ &\quad + P_0 N T_P W(Nr/N) \\ &= P_0 T_P W(r/N) N(N+1)/2 \end{aligned} \tag{17}$$

For a direct capture strategy, the total energy consumption is:

$$\begin{aligned} E_{dir} &= P_0 T_P W(r/N) + P_0 T_P W(2r/N) + \ldots \\ &\quad + P_0 T_P W(Nr/N) \\ &= P_0 T_P \sum_{i=1}^{N} W(ir/N) \end{aligned} \tag{18}$$

As mentioned above, the UASN is divided into different layers, each layer includes many clusters consisting of ordinary and cluster head nodes, and the nodes can adjust their sensing areas [59]. Therefore, communication between nodes can be divided into two steps: communication between nodes within a cluster and between cluster head nodes. Hence, there are two power control schemes for ordinary and cluster head nodes.

The ordinary nodes only need to communicate with the cluster head in the same layer, which means that the distance within the cluster is not far away. The collisions can be avoided if the transmit power can be adjusted to meet the connectivity requirements between nodes in the cluster. Figures 9 (a) and (b) illustrate two-pair transmissions without and with power control, respectively. Figure 9 (a) shows that nodes A and C send signals to nodes B and D, respectively. Then, communication collisions may occur if the power is not restricted and the communication range is not controlled. Assuming that the appropriate transmission power can be selected, the transmission range of the signal can be controlled and maintained with some redundancy to avoid mutual influence and interference, as shown in Figure 9 (b). Hence, the power consumption of the node can be significantly reduced, and its service time can be extended.

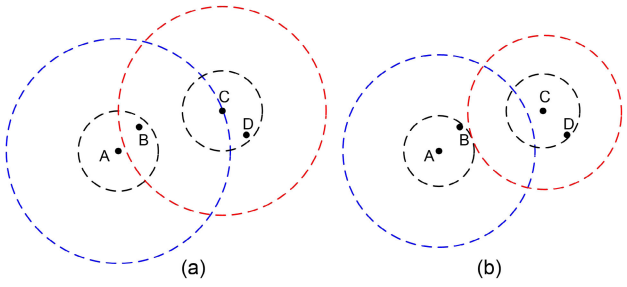

FIGURE 9. Two-pair transmissions: (a) Without power control; (b) With power control.

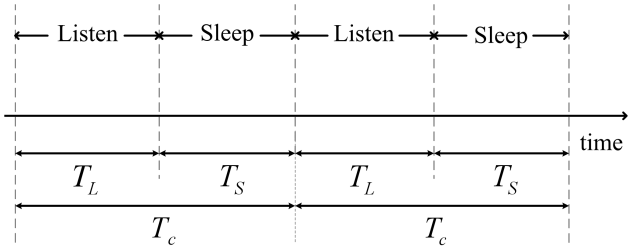

FIGURE 10. Listening and sleeping periodically.

The head node of the cluster is also a relay node that is responsible for transferring the collected information to the corresponding central node of each layer. Then the central node transmits the information layer by layer to the buoy on the sea surface. Therefore, the transmission power and the transmission radius range of the head node are very small, just like the ordinary node. As a relay node, it is necessary to increase the transmission power after the communication within the cluster is completed. The relay node expands the communication range and establishes a communication network with other relay nodes.

E. SLEEPING MODEL OF THE UASN

The UASN usually needs to be used with other detection methods, and it is not always in operation. Hence, the node will be idle for a long time if there is no aware event. As shown in Figure 1, the work efficiency of the idle state is very low, but the energy consumption is high. Therefore, sleep mode is adopted in which only the monitoring function is retained, and other devices are paused to reduce energy consumption [60].

In the monitoring process, each ordinary node regularly runs in sleeping mode to reduce idle and wasted energy. Specifically, all ordinary nodes have the same listening and sleep times, and each ordinary node randomly selects its schedule. Any ordinary node will periodically listen and hibernate if it does not communicate with its neighbor.

It is assumed that nodes in the same layer can achieve synchronous communication, and similar nodes in the same layer can simultaneously listen and sleep to minimize energy consumption without affecting the functionality of the system. Figure 10 shows a timing diagram for the monitoring process. The nodes wake up and sleep regularly during this phase. The listening/sleeping mode is a cycle. Each loop (denoted as T_c) consists of two parts: listening window T_L and sleep window T_S. Hence, $T_c = T_L + T_S$.

F. OVERVIEW OF TDTSPC-MAC PROTOCOL

Figure 11 illustrates the specific process of the proposed TDTSPC-MAC protocol. Firstly, the terrestrial base station communicates with the buoy through the satellite or communication vessel. There is a central node at the center of each layer, just below the buoy. The buoy collects the data information by communicating with these vertical central nodes. Each central node is also responsible for collecting

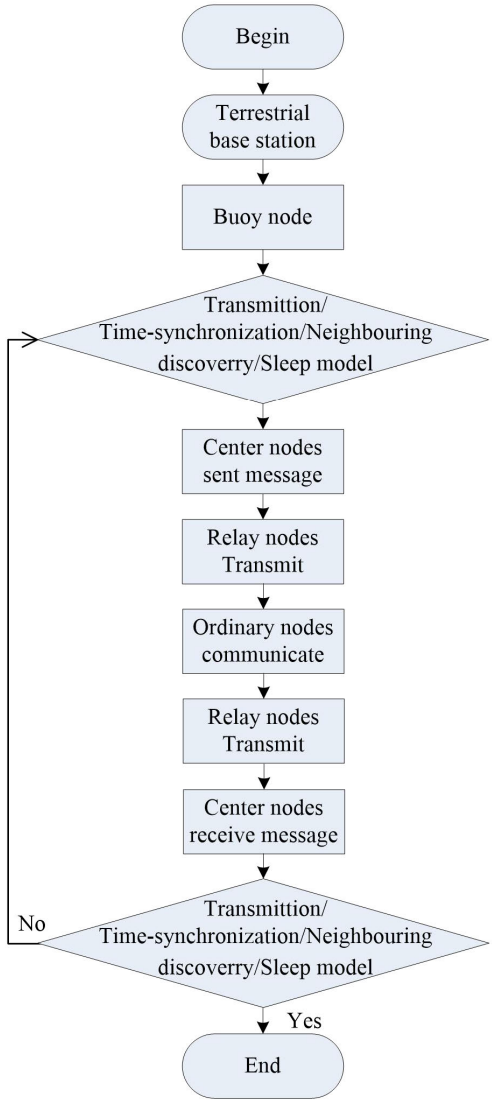

FIGURE 11. Specific process of the proposed TDTSPC-MAC protocol.

information from relay nodes in the same layer. The relay nodes collect data from ordinary sensor nodes in the form of clusters.

The terrestrial base station will quote the standard time after the UASN is completed. Then, synchronization of the nodes can be done in the form of buoy-center-relay-ordinary nodes. There is also a data acquisition and transmission process in which the base station sends a data acquisition command. The ordinary sensor nodes collect relevant data transmitted to the terrestrial base station through the relay and central nodes. Finally, the base station sends an instruction to put the UASN in a monitoring/sleeping state after completing the transmission.

V. COLLISION AVOIDANCE DESIGN OF THE TDTSPC-MAC PROTOCOL

In this phase of the design, the main objective is to enable every node to access the media without collisions. The model

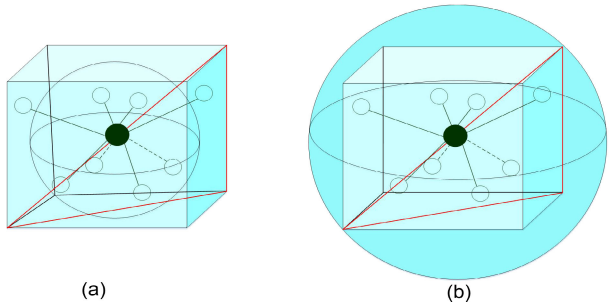

FIGURE 12. Cluster in a cell: (a) Endo-stereoscopic distribution; (b) External stereo distribution.

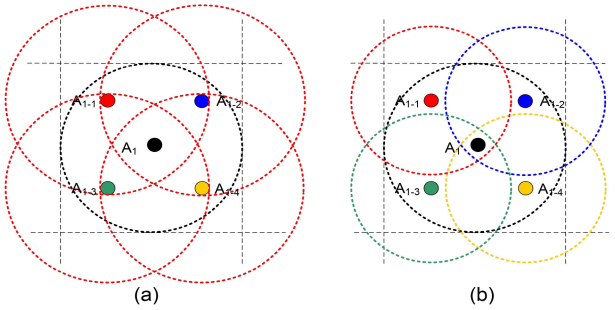

FIGURE 13. Power control in the endo-stereoscopic cluster: (a) Collision; (b) Collision-avoided.

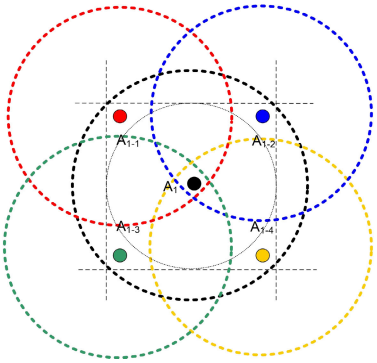

FIGURE 14. Power control in the external stereo cluster.

uses the concepts of hierarchical structures and distributed clustering algorithms to resolve any possible vertical and horizontal collisions.

A. COLLISION AVOIDANCE

Horizontal collisions: Horizontal collisions can be resolved through clustering and power control of each layer. The distributed clustering method allows the cluster head nodes to select sub-frames that should differ from their adjacent clusters. Therefore, the nodes in adjacent clusters can transmit without collision. Moreover, some nodes in the cluster use the handshake protocol to communicate with the cluster header.

Vertical collisions: Vertical collisions can be resolved by dividing the network area into multiple layers, allocating time slots, and controlling power. Specifically, the network can be divided into layer types A, B, and C, and each layer can be divided into different clusters. Two adjacent clusters have different transfer times during the operational phase, while two non-adjacent clusters transmit simultaneously. In addition, different layers are separated from each other in the cluster through power control and timestamp to eliminate vertical collisions between nodes in adjacent layers.

B. COLLISION AVOIDANCE WITHIN A CLUSTER

A three-dimensional clustering topology is used to avoid communication collisions within a cluster. Figure 12 shows the distribution of nodes inside a cell cube. Figure 12 (a) shows that all nodes are distributed inside the cell cube, but some are outside the embedded circle, called endo-stereoscopic distribution. It is assumed that the inscribed circle is the communication range of the cluster head node. The nodes cannot be clustered when distributed in the space between the inscribed circle and the cube. Figure 12 (b) shows that all nodes are distributed within a cube and a circumscribed circle, called the external stereo distribution. Assuming that the circumscribed circle is the communication range of the cluster head. The interactive communication within the cluster can be realized if the communication radius of ordinary nodes is also less than the radius of the cluster head.

Figure 13 shows the power control in the clustering structure of endo-stereoscopic distribution.Figure 13 (a) shows that the ordinary and cluster head nodes within the endo-stereoscopic cluster may still collide, even if the power is controlled. In contrast, the collisions can be avoided, the communication in the network can be carried out in an orderly manner, and the energy consumption can be saved to some extent by controlling the power of the cluster node and assigning a timestamp to each ordinary node in the cluster, as shown in Figure 13 (b). Figure 14 shows that controlling the power and assigning timestamps can also avoid collisions when the nodes are distributed in the space between the inscribed circle and the cube.

The collisions between the ordinary and cluster head nodes can be avoided by assigning different timestamps to the nodes in the cluster after time synchronization and hierarchical clustering of each node. The specific process of intra-cluster communication is shown in Figure 15.

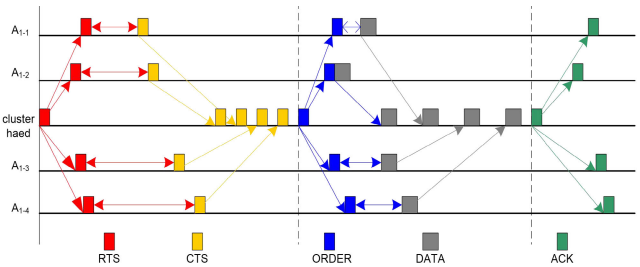

FIGURE 15. Basic procedure of one hope MAC protocol in the cluster.

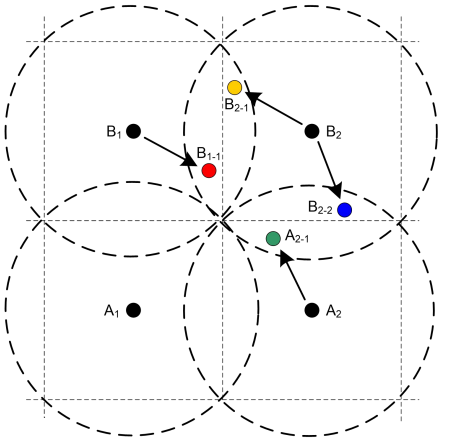

FIGURE 16. Collision between clusters.

C. COLLISION AVOIDANCE BETWEEN CLUSTERS

As mentioned earlier, three-dimensional space is divided into different layers of cell cube space. The power is controlled and time slots are allocated to ensure proper communication within the cluster to realize the connection between the cluster head node and the cluster nodes within the cell space. However, collisions may occur when two adjacent cell spaces (vertically or horizontally) communicate simultaneously. Figure 16 illustrates an example of the collision between clusters. It can be seen that horizontal collisions between adjacent clusters may occur when cluster heads B_1 and B_2 communicate with nodes $B_{1\text{-}1}$ and $B_{2\text{-}1}$, respectively. Similarly, vertical collisions between adjacent clusters may occur when cluster heads A_2 and B_2 communicate with nodes $A_{2\text{-}1}$ and $B_{2\text{-}2}$, respectively.

1) AVOIDANCE OF HORIZONTAL COLLISIONS BETWEEN CLUSTERS

Even with power control, the adjacent clusters in the same layer may still have horizontal collisions when communicating simultaneously. To avoid horizontal collisions, the element space on the horizontal plane is first divided into a mesh structure, as shown in Figure 17. All adjacent clusters are scheduled to run in different timestamps of the same layer according to time synchronization. In Figure 17, each color represents a different time stamp. The specific process is as follows: taking cluster head node A as an example. First, a timestamp is assigned to cluster head node A, and then the same timestamp is arranged for its adjacent cluster head nodes A_1, A_3, A_2, and A_4. By analogy, different timestamps are arranged for all adjacent clusters in the grid so that clusters with the same timestamps can communicate in the same layer at the same time without collision. Therefore, the inter-cluster collision in the horizontal layer can be avoided by allocating the time slot and controlling the power of the node.

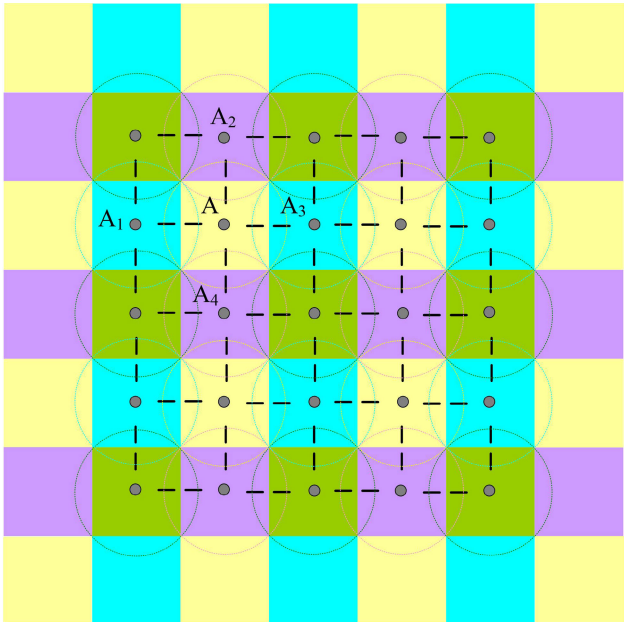

FIGURE 17. Avoidance of horizontal collisions between clusters.

2) AVOIDANCE OF VERTICAL COLLISIONS BETWEEN CLUSTERS

The depth of the node varies slightly due to the anchoring or floating depth in the underwater environment. It is assumed that the UASN is vertically divided into three layers. Thus, when vertically adjacent clusters of different layers communicate simultaneously, vertical collisions can occur between clusters even if the node power is controlled. However, timestamp division based on time synchronization can avoid vertical collisions. Figure 18 shows vertical collision avoidance between clusters in the three layers. The first and third layers are assigned the same timestamp, different from the middle layer, so the adjacent layers can communicate at different periods. Therefore, assigning different timestamps to adjacent layers and controlling the power of each node can avoid vertical cluster collisions.

Aiming at the application scenarios of three-dimensional UASN, a hierarchical clustering structure is proposed. Within the cluster, collision-free communication between the cluster head node and the nodes within the cluster can be implemented. Between clusters, horizontal and vertical communication will not interfere with each other. In this way, the timestamp and power control scheme after time synchronization can effectively avoid collisions, realize the communication between ordinary and relay nodes, and maintain certain communication redundancy.

D. COLLISION AVOIDANCE BETWEEN CLUSTER HEAD NODES

Figure 19 illustrates the cluster head nodes connectivity in a layer. The center node is located at the center of each floor, directly below the buoy node. After intra-cluster communication, the information collected by sensors will be transmitted

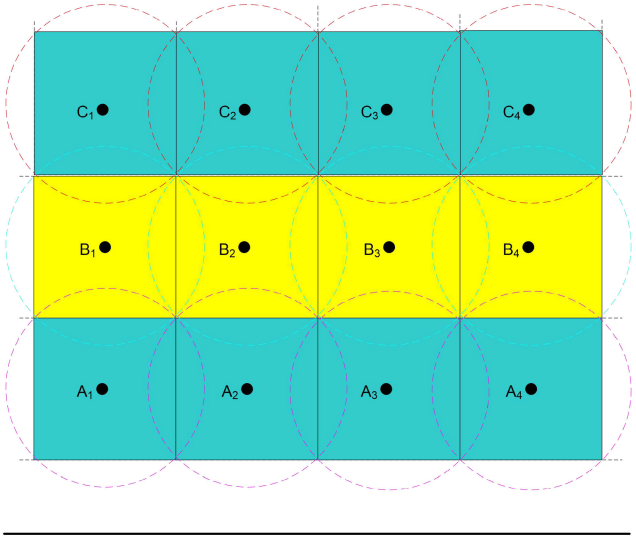

FIGURE 18. Avoidance of vertical collisions between clusters.

from ordinary nodes in the cluster to the head nodes. Then, the cluster head node transmits the information to the central node of each layer in multiple hops when the information is collected. The central node of each layer transmits the collected information to the buoy nodes on the sea surface layer by layer. Therefore, a power control mechanism is designed for the cluster head nodes. Specifically, cluster head (relay) nodes can change the communication position through power control and realize small-scale intra-cluster and large-scale inter-cluster communication, thus ensuring the normal communication of UASN.

1) AVOIDANCE OF HORIZONTAL COLLISIONS BETWEEN CLUSTER HEAD NODES

The data flow between cluster head nodes is also marked in Figure 19. To avoid collisions, two adjacent processes are arranged to execute in two consecutive periods. In the first stage, the outermost relay nodes transmit the collected information to the inner relay nodes. In the second stage, the inner relay nodes transmit data to the central node in each layer through single-hop communication. The process of the second stage is similar to the intra-cluster node communication in Figure 15. Figure 20 illustrates the avoidance

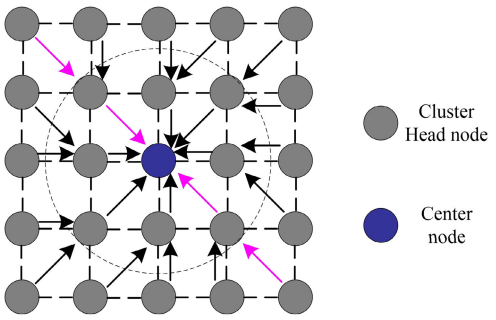

FIGURE 19. Cluster head nodes connectivity in a layer.

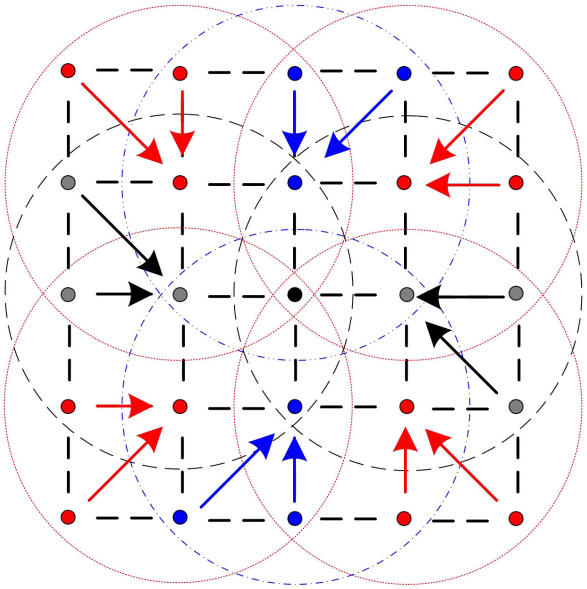

FIGURE 20. Avoidance of horizontal collisions between cluster head (relay) nodes.

of horizontal collisions between cluster head nodes. In the first stage, the inner node is used as the cluster head to form a cluster with two different outer nodes. These clusters are divided into three categories, corresponding to different time gaps. Since the position of each node is relatively fixed, the communication radius of each node is fixed after determining the transmission power. After time and space re-planning, collision-free communication between relay nodes on the horizontal plane can be realized.

2) AVOIDANCE OF VERTICAL COLLISIONS BETWEEN CLUSTER HEAD NODES

Following the pink arrow in Figure 19 and taking its plan view as an example to explain the vertical collision avoidance between cluster head nodes while communicating. The central nodes are responsible for transmitting the data collected by relay nodes on the same floor to the buoy node on the sea surface layer by layer. Moreover, the relay nodes in the same layer transmit data to the central node through other relay nodes hop by hop. In this process, collisions may occur.

It is assumed that the relay node can control the transmission power and realize intra-cluster and inter-cluster communication in a small range and a large range, respectively. Since the location of the relay node is fixed, its communication range is relatively stable. The relay nodes are evenly distributed in three layers in the three-dimensional space, as shown in Figure 21. The relay nodes in layers A and C are assigned the same communication time slot, while the relay node in layer B works in a different time slot. Therefore, there will be no vertical communication collisions in each layer of relay communication.

Figure 22 shows that the center nodes are arranged at intervals along the vertical center line of the buoy to facilitate data acquisition and transmission. Specifically, the center

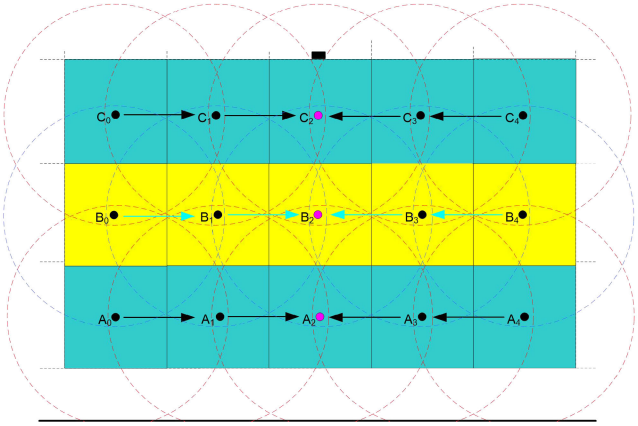

FIGURE 21. Avoidance of vertical collisions between cluster head nodes.

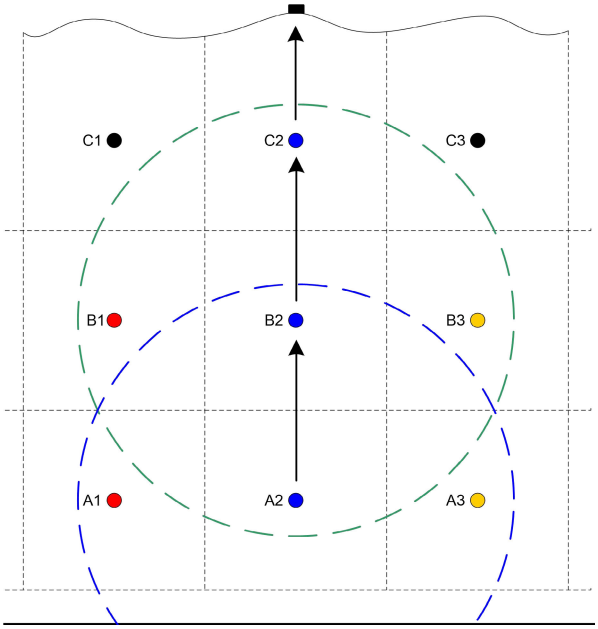

FIGURE 22. Transmitted data in center nodes layer by layer.

nodes need to upload the information layer by layer to the buoy nodes on the sea surface and transmit the information to the terrestrial base station through the radio of the buoy after collecting the data from the relay nodes in the same layer.

Since the network is vertical communication of the central node, there is no horizontal connection. Therefore, a hierarchical handshake protocol is designed to achieve reliable information transmission between the buoy and central node, as shown in Figure 23.

In summary, the vertical collision of underwater acoustic communication can be avoided through time synchronization, power control strategy, and distributed clustering of single-hop adjacent nodes. Moreover, the horizontal collision between nodes can be eliminated in different layers.

VI. PERFORMANCE EVALUATION

This section first describes the simulation parameters of the protocol and specifies the metrics used to evaluate the performance of the proposed TDTSPC-MAC protocol. Then, the simulation results are presented and analyzed, and the performance of the TDTSPC-MAC protocol is discussed. Finally, the TDTSPC-MAC protocol is quantitatively compared with three existing protocols.

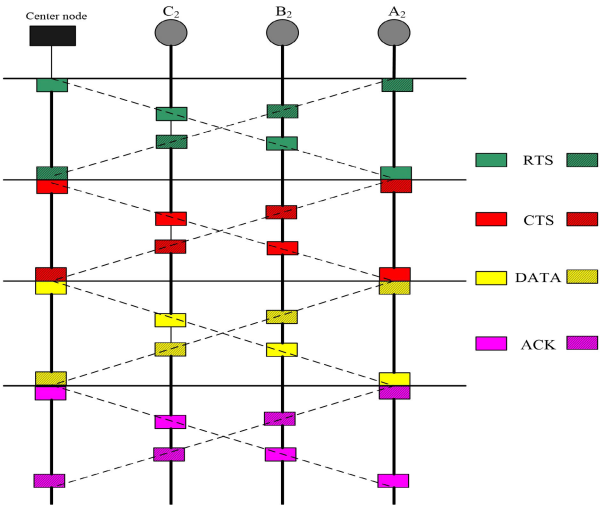

FIGURE 23. Basic procedure of TDTSPC protocol in center nodes.

A. SIMULATION PARAMETERS

The ranges of short-distance and long-distance network communications are 90 and 110 meters, respectively. In addition, the bandwidth is set to 15 kHz, and the simulation parameters are listed in Table 1.

TABLE 1. Simulation parameters.

Parameter	Value
Transmission power	2 Watts
Receiver power	0.75Watts
Gross power	8 mW
Maximum propagation distance	150 m
Bandwidth	10 Kb/s
Acoustic propagation speed	1500 m/s
Traffic rate	0.05-0.4 packets/s
Node Number	80-220 sensor nodes
Deployment region	500 m×500 m×300 m
Running rounds	20
Control packet size	60 bits
Data packet size	1000 bits

Specifically, four metrics are defined to compare the performance of the proposed TDTSPC-MAC protocol with SFAMA-MAC [61], TLohi-MAC [62], and CSMA-MAC [63]. The four metrics are delay time, communication time, throughput, and energy consumption. Furthermore, the network throughput is defined by the bits transmitted by packets per second as follows:

$$I_g = \frac{L_g}{D_g} = \frac{\sum_{i \in g} n_i \gamma L_{data} H_i (1 - P_e)^{2L_{data}}}{D_g} \quad (19)$$

where L_g is the total length of a round's packets received correctly by the cluster header node, composed of all packets in the cluster. The bit error rate P_e is related to the specifications of the modem and the characteristics of the underwater acoustic channel. H_i is the average number of packets by cluster i transmitted in one round, which can be calculated as follows:

$$\begin{aligned} H_i &= \sum_{k=1}^{N_i-1} kP^k \\ &= \sum_{k=1}^{N_i-1} kC_{N_i}^k P^k (1-P)^{N_i-k} = N_i P \end{aligned} \tag{20}$$

where N_i represents the total number of nodes in cluster i, and P represents the probability of generating packets in one round, which is defined as:

$$P = 1 - e^{-\lambda D_C} \tag{21}$$

where λ is the data generation rate of a node and D_C is a round of acquisition delay, which consists of the transmission time d_i^t of each cluster and the transmission time d_i^p between clusters.

Finally, the energy consumption of the network consists of transmitted energy, received energy, and idle energy for all nodes. The transmission power is closely related to the transmission frequency and the distance between the acoustic modems. Therefore, the transmission power is adjusted according to the frequency and transmission distance in the model. It is assumed that the received power is fixed. Then, the energy expenditure is defined as:

$$E_g = \sum\nolimits_{i \in g} \left(E_i^t + E_i^r\right) + E_{idle} \tag{22}$$

where the cluster indicator is i, E_i^t is the transmission energy, including the transmission energy of the ordinary nodes and the cluster head node. Thus, the transmission energy can be calculated as follows:

$$E_i^t = \sum\nolimits_{j \in g_i} P_{ij}^t T_{ij}^t = E_{g_i}^t + \sum\nolimits_{j \in g_{ij} \neq g_i} \frac{P_{ij}^t L_{ij}^t}{R} \tag{23}$$

where g_i is the set of nodes in cluster i, and j is the node indicator in the cluster. The transmission power and the transmission time of node j in cluster i are P_{ij}^t and T_{ij}^t, respectively, and the node's packet length in cluster i is L_{ij}^t, which consists of the length of the packet, *i.e.*, $L_{ij}^t = n_i \gamma L_{data}$. The transmission energy $E_{g_i}^t$ of the cluster head node includes WAKE packets, ACK packets, and transmission energy of inter-cluster packets. $E_{g_i}^t$ can be expressed as:

$$E_{g_i}^t = P_{\max}\left(L_{wake} + n_i L_{ack}\right) + \frac{P_{\max} N_i n_i \gamma L_{data}}{R} \tag{24}$$

When the distance reaches the communication distance limit d_0, the transmission power of the cluster head node is $P_{\max}$. E_i^r is the energy received by cluster i, including the energy received by the cluster head node and the ordinary nodes in the cluster. The energy received by the inter-cluster nodes is mainly composed of WAKE and ACK packets. In contrast, the cluster head node's received energy includes the received energy of the packets and the ACTIVE packets. Hence, E_i^r can be calculated as:

$$\begin{aligned} E_i^r &= \sum\nolimits_{j \in g_i} P^r T_{ij}^r = \frac{P^r \left(N_i n_i \gamma L_{data} + L_{active}\right)}{R} \\ &+ \sum\nolimits_{j \in g_{ij} \neq g_i} \frac{P^r L_{g_i}^r \left(L_{wake} + n_i L_{ack}\right)}{R} \end{aligned} \tag{25}$$

where $\left(N_i n_i \gamma L_{data} + L_{active}\right)$ and $L_{g_i}^r \left(L_{wake} + n_i L_{ackz}\right)$ are the received powers of P^r and T_{ij}^r, respectively, and g_i is the received packet length between each intra-cluster node and the cluster head.

$$\begin{aligned} E_{idle} &= P_{idle}\left(D - \frac{L_{C_i}^t + L_{C_i}^r}{R}\right) \\ &+ \sum\nolimits_{j \in g_{ij} \neq g_i} P_{idle}\left(D - \frac{L_{ij}^t + L_{ij}^r}{R}\right) \end{aligned} \tag{26}$$

where $L_{g_i}^r$ is the length of the transmitted packet for the cluster head, and it can be calculated by the formula $L_{g_i}^r = L_{wake} + n_i L_{ack} + N_i n_i \gamma L_{data}$.

B. AVERAGE DELAY FOR DIFFERENT NODES

To analyze and study the scalability of each protocol to the network, the average delay of each protocol is observed by increasing the nodes' number and keeping other conditions the same. Figure 24 shows the average delay of the four protocols for different numbers of nodes. It can be seen from the figure that the average delay time increases with the increase in the number of nodes. That is, the average delay time of all four protocols is inversely proportional to the number of nodes. When the same 60 nodes are used, the average network delay of the TDTSPC-MAC protocol is respectively 82.7% and 81.7% less than that of the CSMA and SFAMA protocols and is 2.3% less than that of the T-Lohi protocol.

As the number of nodes gradually increases, the number of packets of nodes and the number of collisions also increase. Thus, the average delay time of the CSMA, SFAMA and T-Lohi protocols also increases. Since the SFAMA and T-Lohi protocols are designed for the uncertainty of time and space and high delay to avoid collision and re-transmission, the changes of the SFAMA and T-Lohi protocols are not as fast as the CSMA protocol. Moreover, the network delay

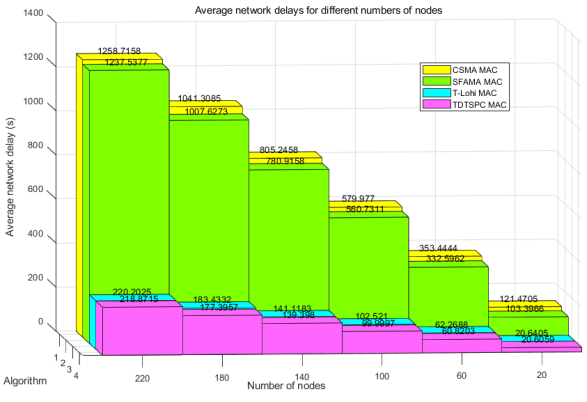

FIGURE 24. Average network delays for different numbers of nodes.

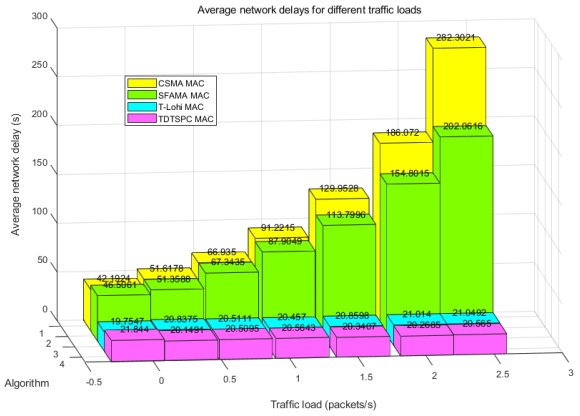

FIGURE 25. Average network delays for different traffic loads.

time increases significantly with the number of nodes in the CSMA protocol because the CSMA protocol has multiple Requests To Send (RTS) frames in the case of multi-hop, which overlap under the uncertainty of time and space, resulting in delay. However, the average delay time of the proposed TDTSPC-MAC protocol increases slowly with the increase in the number of nodes compared with the other three protocols. The simulation results show that the TDTSPC-MAC protocol is slightly better than the T-Lohi protocol in average delay time but far better than the SFAMA and CSMA protocols.

C. AVERAGE DELAY FOR DIFFERENT TRAFFIC LOADS

Next, the average network delays of the four protocols for different loads are compared while keeping the other conditions the same. Figure 25 shows the average network delays of the four protocols. It can be seen that the average network delay time of the proposed TDTSPC-MAC protocol is respectively 60.9%, 60.7%, and 3.3% less than that of the CSMA, SFAMA, and T-Lohi protocols when the traffic load is 0.5 packets/s. The T-Lohi and CSMA protocols cannot effectively detect hidden nodes and space-time uncertainty, which leads to more packet loss, collision, and longer delay times. However, the TDTSPC-MAC and T-Lohi protocols can effectively solve this problem. The average delay difference among the four protocols is not obvious when the traffic is small. Nevertheless, with the increase in traffic, the delay also gradually increases due to the low scheduling efficiency of UASN, resulting in many collisions and re-transmissions.

Simulation results show that the average network delay of the TDTSPC-MAC protocol is much better than that of the CSMA and SFAMA protocols. The TDTSPC-MAC and T-Lohi protocols are designed to avoid collision and re-transmission caused by spatial-temporal uncertainty and high delay. While the average network delay time of the CSMA and SFAMA protocols gradually increases, the traffic is further increased due to the increase in collision time. The sensed channel state is unreliable due to spatial-temporal uncertainty in the high-delay acoustic network. If the CSMA protocol sensing channel is idle at this moment, the node transmits. Otherwise, it will retreat uniformly within the maximum propagation delay to try later.

Thus, the data collision is avoided, and the channel utilization rate of the UASN is significantly improved due to the time synchronization and power control mechanisms in the hierarchical clustering structure. The average delay time of the TDTSPC-MAC protocol changes slightly with the increase of the nodes. Moreover, the TDTSPC-MAC protocol has the best utilization under high load because cycling is the best strategy when all nodes are saturated. However, the T-Lohi protocol provides higher channel utilization before the channel begins to saturate because the contention-based channel access provides a much lower delay. Both T-Lohi and TDTSPC-MAC protocols are stable when the channel is overloaded.

D. DATA TRANSMISSION THROUGHPUT FOR DIFFERENT TRAFFIC LOADS

The third simulation evaluates the impact of the load on the throughput of four protocols with 100 sensor nodes. Figure 26 compares the data transmission throughputs of the four protocols for different traffic loads. It can be seen from the figure that the network throughput increases correspondingly and finally reaches saturation when the provided traffic increases. The simulation results show that the network throughput performance of the proposed TDTSPC-MAC protocol is better than the other three protocols.

When the packet generation rate is low, data-string transmission rarely occurs in SFAMA protocol, and multiple RTS attempts hardly occur. However, when the packet generation rate increases, the problem of multiple RTS attempts in SFAMA becomes more serious. Moreover, the SFAMA protocol suffers throughput degradation when the traffic volume increases. Since the protocol SFAMA does nothing but back off when multiple RTS attempt problems occur, the high-frequency back-off significantly limits the throughput. The CSMA protocol does not consider the uncertainty of time and space in UASN, and its network throughput is far lower than the other three media access control protocols. The T-Lohi protocol takes advantage of the uncertainty of

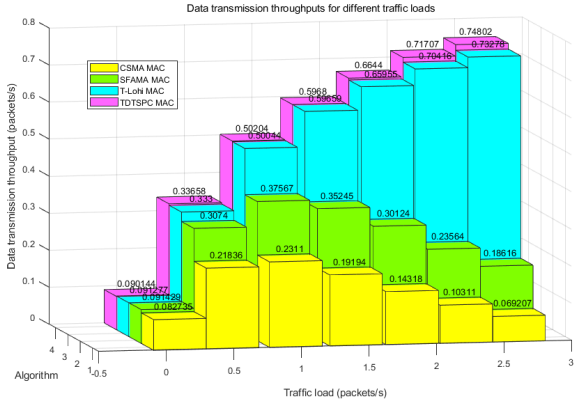

FIGURE 26. Data transmission throughputs for different traffic loads.

time and space and high delay to avoid collision and re-transmission. Under the same traffic load condition, the proposed TDTSPC-MAC protocol adopts the hierarchical cluster structure, which can avoid communication collisions through a time synchronization scheme and power control strategy, thus improving network throughput.

E. AVERAGE TRAFFIC TIME FOR DIFFERENT NODES

Next, the fourth simulation test studies the influence of the sensor nodes on the communication time of the four protocols. Figure 27 compares the average traffic times of the four protocols for different numbers of nodes. It can be seen from the figure that the network traffic time of CSMA and SFAMA protocols increases with the deployment of nodes, especially for the CSMA protocol. When the same 140 nodes are used, the network traffic time of the TDTSPC-MAC protocol is respectively 92.7% and 89.8% less than that of the CSMA and SFAMA protocols and is 2.3% less than that of the T-Lohi protocol.

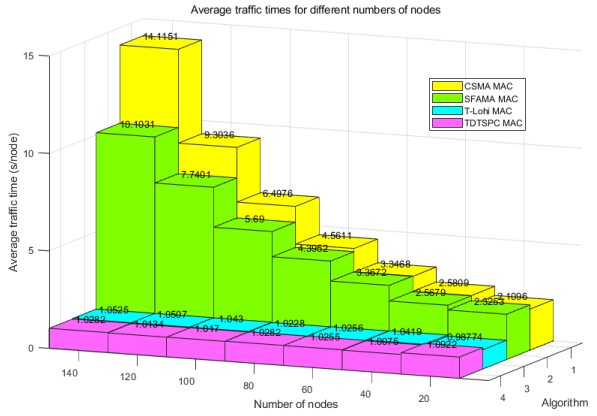

FIGURE 27. Average traffic times for different numbers of nodes.

Since multiple RTS attempts in CSMA protocol exist, these RTS overlap in the time domain due to long underwater propagation delay. Moreover, considering the uncertainty of underwater time and space, the other three MAC protocols avoid collisions when deploying the same nodes and have lower network traffic time. The SFAMA protocol achieves higher throughput than the CSMA protocol. Since more data packets are transmitted through the data link when the traffic volume increases, the longer data link will replace the shorter data link. The T-Lohi protocol finds a way to deal with the high delay caused by underwater time and space uncertainty. It allocates time slots to the sender, and the duration of time slots is equal to the packet transmission time plus the maximum propagation delay, thus reducing collisions and re-transmissions compared with CSMA and SFAMA protocols. Finally, the proposed TDTSPC-MAC protocol adopts a hierarchical clustering structure, which can prevent communication collisions through time synchronization and power control, thus reducing the network traffic time.

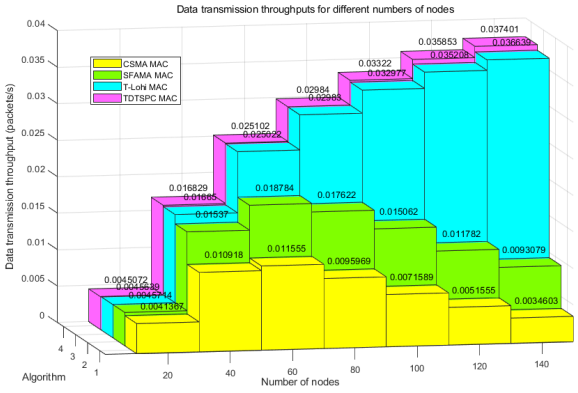

FIGURE 28. Data transmission throughputs for different numbers of nodes.

F. AVERAGE THROUGHPUT FOR DIFFERENT NODES

The fifth simulation test studies the influence of the number of sensor nodes on the throughput of the four protocols. Figure 28 shows the average data transmission throughputs of the four protocols for different node densities. It can be observed that the network throughputs of the proposed TDTSPC-MAC and T-Lohi protocols increase with the increase in the number of nodes. On the contrary, the throughputs of CSMA and SFAMA protocols gradually decrease with the increase in the number of nodes after reaching the peak.

Since the CSMA protocol does not consider the irregularity of underwater time and space, its network traffic time is longer than the other three MAC protocols. The nodes in SFAMA use multiple RTS attempts to complete data transmission through the sorted data strings. Thus, more data packets can be transmitted during each round of simultaneous handshake because more useful data transmission can be successfully transmitted when the traffic volume in SFAMA becomes higher. However, the throughput of the SFAMA protocol also decreases with the increase in the nodes because the problem of multiple RTS attempts becomes more serious with the increase in the network density. Compared with the CSMA protocol, the T-Lohi protocol effectively deals with the high delay caused by underwater time and space uncertainty, thus reducing collision and re-transmission. Since the proposed TDTSPC-MAC protocol adopts a hierarchical cluster structure that can prevent communication collisions through time synchronization and power control, network traffic time is significantly reduced.

G. ENERGY CONSUMPTION FOR DIFFERENT OFFERED TRAFFIC LOADS

The sixth simulation evaluates the influence of different loads on the energy consumption of the four protocols. Figure 29 shows the energy per bit of the four protocols for different traffic loads. It can be seen from the figure that energy per bit of CSMA and SFAMA protocols increases with the load, especially for the CSMA protocol. When the traffic load is two packets/s, the network energy consumption of the

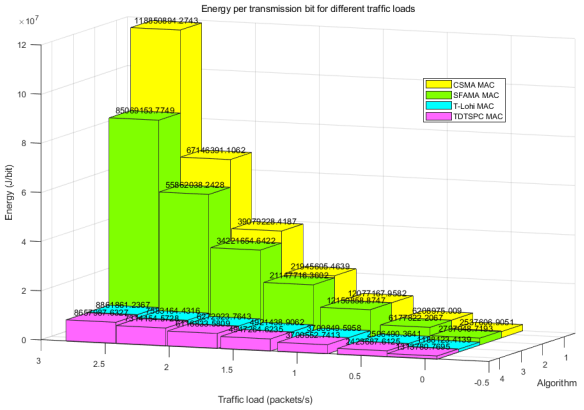

FIGURE 29. Energy per transmission bit for different traffic loads.

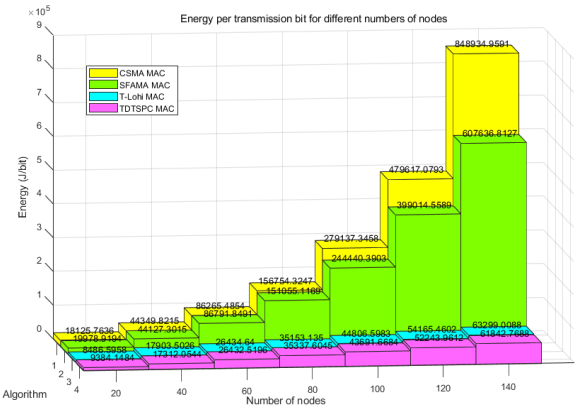

FIGURE 30. Energy per transmission bit for different numbers of nodes.

TDTSPC-MAC protocol is respectively 84.3% and 82.1% lower than that of the CSMA and SFAMA protocols and is 2.4% lower than that of the T-Lohi protocol. Since the CSMA protocol does not consider the uncertainty of underwater time and space, its energy consumption is higher than the other three MAC protocols. Since the proposed TDTSPC-MAC and T-Lohi protocols take the underwater space-time uncertainty into account, they have lower energy consumption under the same load. Besides, the SFAMA protocol reduces collision and re-transmission to some extent due to the addition of a time-sharing mechanism, and its energy consumption is better than the CSMA protocol. The results demonstrate that the proposed TDTSPC-MAC protocol is the most energy efficient among the four protocols.

H. AVERAGE POWER CONSUMPTION

Once the transmission bandwidth is set, the transmission power $p(l)$ can be adjusted to achieve the required 3dB bandwidth $B_{3dB}(l)$ corresponding to the narrowband signal-to-noise ratio (SNR) level. If $S_l(f)$ is used to represent the power spectral density (PSD) of the transmitted signal at distance l, the total transmitted power is expressed as [64]:

$$p(l) = \int_{B_{3dB}(l)} S_l(f)df = SNR_0 B_{3dB}(l) \frac{\int_{B_{3dB}(l)} N(f)df}{\int_{B_{3dB}(l)} A^{-1}(l,f)df} \quad (27)$$

Among them, the spectral density of the transmitted signal power can be regarded as a constant value.

Finally, the seventh simulation evaluates the influence of increasing the number of protocol nodes on energy consumption under the condition of constant traffic. Figure 30 shows the energy per transmission bit of the four protocols for different numbers of nodes. It can be seen that the energy consumption of the four protocols increases with the number of nodes. When the same 120 nodes are used, the energy per transmission bit of the TDTSPC-MAC protocol is respectively 89.1% and 86.9% lower than that of the CSMA and SFAMA protocols and is 3.5% lower than that of the T-Lohi protocol. Energy consumption also rises with the collisions increase. Since more sensors are involved in the network with the increase of nodes, the competition for access channels becomes more and more fierce. The proposed TDTSPC-MAC protocol considers the uncertainty of hidden terminal and space-time and takes energy-saving measures. Therefore, the TDTSPC-MAC protocol consumes the least energy among the four protocols. Compared with CSMA and SFAMA protocols, the T-Lohi protocol uses the wake-up sound receiver to save energy, which monitors the wake-up sound with low power. Thus, the T-Lohi protocol consumes much less energy than the CSMA and SFAMA protocols.

VII. CONCLUSION

This paper proposes a MAC protocol called TDTSPC-MAC based on time synchronization and power control to avoid communication collisions and save energy consumption for UASNs deployed in three-dimensional space. Firstly, the energy consumption of sensor nodes is analyzed, focusing on communication collision and standby. The three-dimensional underwater space can be effectively divided and monitored through nodes' hierarchical and clustering design. Collision-free communication can be effectively realized through time synchronization and power control strategy. Moreover, the monitoring and sleeping mode periodically makes the nodes sleep when idle, saving energy. The proposed TDTSPC-MAC protocol is suitable for underwater acoustic sensor networks and can be used to monitor the position and movement of underwater vehicles. The simulation results demonstrate and validate that the proposed TDTSPC-MAC protocol has good energy consumption, throughput, and delay time performance compared with the existing protocols. In future works, the authors will consider applying the proposed MAC protocol to the dynamic deep-sea environment.

ACKNOWLEDGMENT

The authors would like to thank all the anonymous reviewers for their valuable comments and suggestions.

REFERENCES

[1] G. Yang, L. Dai, and Z. Wei, "Challenges, threats, security issues and new trends of underwater wireless sensor networks," *Sensors*, vol. 18, no. 11, p. 3907, 2018.

[2] A. Al Guqhaiman, O. Akanbi, A. Aljaedi, and C. E. Chow, "A survey on MAC protocol approaches for underwater wireless sensor networks," *IEEE Sensors J.*, vol. 21, no. 3, pp. 3916–3932, Feb. 2021.

[3] J. Qiu, Z. Xing, C. Zhu, K. Lu, J. He, Y. Sun, and L. Yin, "Centralized fusion based on interacting multiple model and adaptive Kalman filter for target tracking in underwater acoustic sensor networks," *IEEE Access*, vol. 7, pp. 25948–25958, 2019.

[4] R. Zhang, X. Cheng, X. Cheng, and L. Yang, "Interference-free graph based TDMA protocol for underwater acoustic sensor networks," *IEEE Trans. Veh. Technol.*, vol. 67, no. 5, pp. 4008–4019, May 2018.

[5] Y. Song and P.-Y. Kong, "Optimizing design and performance of underwater acoustic sensor networks with 3D topology," *IEEE Trans. Mobile Comput.*, vol. 19, no. 7, pp. 1689–1701, Jul. 2020.

[6] A. Stefanov and M. Stojanovic, "Design and performance analysis of underwater acoustic networks," *IEEE J. Sel. Areas Commun.*, vol. 29, no. 10, pp. 2012–2021, Dec. 2011.

[7] T. Northardt, "A Cramér-rao lower bound derivation for passive sonar track-before-detect algorithms," *IEEE Trans. Inf. Theory*, vol. 66, no. 10, pp. 6449–6457, Oct. 2020.

[8] Y. Su, Z. Zhou, Z. Jin, and Q. Yang, "A joint relay selection and power allocation MAC protocol for underwater acoustic sensor network," *IEEE Access*, vol. 8, pp. 65197–65210, 2020.

[9] L. Pu, Y. Luo, H. Mo, S. Le, Z. Peng, J.-H. Cui, and Z. Jiang, "Comparing underwater MAC protocols in real sea experiments," *Comput. Commun.*, vol. 56, pp. 47–59, Feb. 2015.

[10] M. Al Ameen, S. M. R. Islam, and K. Kwak, "Energy saving mechanisms for MAC protocols in wireless sensor networks," *Int. J. Distrib. Sensor Netw.*, vol. 6, no. 1, Jan. 2010, Art. no. 163413.

[11] S. Karim, F. K. Shaikh, K. Aurangzeb, B. S. Chowdhry, and M. Alhussein, "Anchor nodes assisted cluster-based routing protocol for reliable data transfer in underwater wireless sensor networks," *IEEE Access*, vol. 9, pp. 36730–36747, 2021.

[12] G. Tuna and V. C. Gungor, "A survey on deployment techniques, localization algorithms, and research challenges for underwater acoustic sensor networks," *Int. J. Commun. Syst.*, vol. 30, no. 17, p. e3350, Jun. 2017.

[13] C. Hsu, K. C.-J. Lin, Y.-R. Lai, and C.-F. Chou, "On exploiting spatial–temporal uncertainty in max-min fairness in underwater sensor networks," *IEEE Commun. Lett.*, vol. 14, no. 12, pp. 1098–1100, Dec. 2010.

[14] O. Pallares, P.-J. Bouvet, and J. Del Rio, "TS-MUWSN: Time synchronization for mobile underwater sensor networks," *IEEE J. Ocean. Eng.*, vol. 41, no. 4, pp. 763–775, Oct. 2016.

[15] J. Xu, K. Li, G. Min, K. Lin, and W. Qu, "Energy-efficient tree-based multipath power control for underwater sensor networks," *IEEE Trans. Parallel Distrib. Syst.*, vol. 23, no. 11, pp. 2107–2116, Nov. 2012.

[16] S. Poudel and S. Moh, "Energy-efficient and fast MAC protocol in UAV-aided wireless sensor networks for time-critical applications," *Sensors*, vol. 20, no. 9, p. 2635, May 2020.

[17] W. Zhang, J. Wang, G. Han, X. Zhang, and Y. Feng, "A cluster sleep-wake scheduling algorithm based on 3D topology control in underwater sensor networks," *Sensors*, vol. 19, no. 1, p. 156, Jan. 2019.

[18] K. Chen, E. Cheng, F. Yuan, W. Su, and M. Ma, "The influence of MAC protocol on a non-synchronous localization scheme in large-scale UWSNs," *IEEE Access*, vol. 6, pp. 16386–16394, 2018.

[19] S. C. Dhongdi, P. Nahar, R. Sethunathan, L. J. Gudino, and K. R. Anupama, "Cross-layer protocol stack development for three-dimensional underwater acoustic sensor network," *J. Netw. Comput. Appl.*, vol. 92, pp. 3–19, Aug. 2017.

[20] D. Pompili, T. Melodia, and I. F. Akyildiz, "Three-dimensional and two-dimensional deployment analysis for underwater acoustic sensor networks," *Ad Hoc Netw.*, vol. 7, no. 4, pp. 778–790, Jun. 2009.

[21] K. Zhang, J. Du, J. Wang, C. Jiang, Y. Ren, and A. Benslimane, "Distributed hierarchical information acquisition systems based on AUV enabled sensor networks," in *Proc. IEEE Int. Conf. Commun. (ICC)*, Shanghai, China, May 2019, pp. 1–6.

[22] L. Liu, Y. Liu, and N. Zhang, "A complex network approach to topology control problem in underwater acoustic sensor networks," *IEEE Trans. Parallel Distrib. Syst.*, vol. 25, no. 12, pp. 3046–3055, Dec. 2014.

[23] F. A. Alfouzan, A. Shahrabi, S. M. Ghoreyshi, and T. Boutaleb, "A collision-free graph coloring MAC protocol for underwater sensor networks," *IEEE Access*, vol. 7, pp. 39862–39878, 2019.

[24] F. A. Alfouzan, A. Shahrabi, S. M. Ghoreyshi, and T. Boutaleb, "An energy-conserving collision-free MAC protocol for underwater sensor networks," *IEEE Access*, vol. 7, pp. 27155–27171, 2019.

[25] F. Ahmed and H.-S. Cho, "A time-slotted data gathering medium access control protocol using Q-learning for underwater acoustic sensor networks," *IEEE Access*, vol. 9, pp. 48742–48752, 2021.

[26] N. Morozs, P. D. Mitchell, and R. Diamant, "Scalable adaptive networking for the Internet of Underwater Things," *IEEE Internet Things J.*, vol. 7, no. 10, pp. 10023–10037, Oct. 2020.

[27] G. Xing, Y. Chen, R. Hou, M. Dong, D. Zeng, J. Luo, and M. Ma, "Game-theory-based clustering scheme for energy balancing in underwater acoustic sensor networks," *IEEE Internet Things J.*, vol. 8, no. 11, pp. 9005–9013, Jun. 2021.

[28] K. R. Anupama, A. Sasidharan, and S. Vadlamani, "A location-based clustering algorithm for data gathering in 3D underwater wireless sensor networks," in *Proc. Int. Symp. Telecommun.*, Tehran, Iran, Aug. 2008, pp. 343–348.

[29] J. Yi, D. Mirza, R. Kastner, C. Schurgers, P. Roberts, and J. Jaffe, "TOA-TS: Time of arrival based joint time synchronization and tracking for mobile underwater systems," *Ad Hoc Netw.*, vol. 34, pp. 211–223, Nov. 2015.

[30] Z. Jin, S. Xiao, Y. Su, and Y. Li, "PC-MAC: A prescheduling and collision-avoided MAC protocol for underwater acoustic sensor networks," *J. Sensors*, vol. 2017, Dec. 2017, Art. no. 4209301.

[31] C. Li, Y. Xu, Q. Wang, B. Diao, Z. An, Z. Chen, and Z. Luo, "FDCA: A full-duplex collision avoidance MAC protocol for underwater acoustic networks," *IEEE Sensors J.*, vol. 16, no. 11, pp. 4638–4647, Jun. 2016.

[32] J. Liu, Z. Wang, J.-H. Cui, S. Zhou, and B. Yang, "A joint time synchronization and localization design for mobile underwater sensor networks," *IEEE Trans. Mobile Comput.*, vol. 15, no. 3, pp. 530–543, Mar. 2016.

[33] P. Wang, C. Y. Li, J. Zheng, and H. T. Mouftah, "A dependable clustering protocol for survivable underwater sensor networks," in *Proc. IEEE Int. Conf. Commun.*, Beijing, China, May 2008, pp. 3263–3268.

[34] Z. Gong, C. Li, and F. Jiang, "AUV-aided joint localization and time synchronization for underwater acoustic sensor networks," *IEEE Signal Process. Lett.*, vol. 25, no. 4, pp. 477–481, Apr. 2018.

[35] D. Kim, J. Jung, Y. Koo, and Y. Yi, "Bird-MAC: Energy-efficient MAC for quasi-periodic IoT applications by avoiding early wake-up," *IEEE Trans. Mobile Comput.*, vol. 19, no. 4, pp. 788–802, Apr. 2020.

[36] M. Wang, Y. Chen, X. Sun, F. Xiao, and X. Xu, "Node energy consumption balanced multi-hop transmission for underwater acoustic sensor networks based on clustering algorithm," *IEEE Access*, vol. 8, pp. 191231–191241, 2020.

[37] S. Lmai, M. Chitre, C. Laot, and S. Houcke, "Throughput-efficient super-TDMA MAC transmission schedules in ad hoc linear underwater acoustic networks," *IEEE J. Ocean. Eng.*, vol. 42, no. 1, pp. 156–174, Jan. 2017.

[38] Y. Su, R. Fan, Z. Jin, and X. Fu, "Design of an OFDMA-based MAC protocol for an underwater glider network with motion prediction," *IEEE Access*, vol. 6, pp. 62655–62663, 2018.

[39] F. Zhou, Q. Wang, G. Han, G. Qiao, Z. Sun, and A. Niaz, "APE-Sync: An adaptive power efficient time synchronization for mobile underwater sensor networks," *IEEE Access*, vol. 7, pp. 52379–52389, 2019.

[40] Y. Su, Y. Zhu, H. Mo, J.-H. Cui, and Z. Jin, "A joint power control and rate adaptation MAC protocol for underwater sensor networks," *Ad Hoc Netw.*, vol. 26, pp. 36–49, Mar. 2015.

[41] L. Qian, S. Zhang, M. Liu, and Q. Zhang, "A MACA-based power control MAC protocol for underwater wireless sensor networks," in *Proc. IEEE/OES China Ocean Acoust. (COA)*, Harbin, China, Jan. 2016, pp. 1–8.

[42] X. Guo, M. R. Frater, and M. J. Ryan, "Design of a propagation-delay-tolerant MAC protocol for underwater acoustic sensor networks," *IEEE J. Ocean. Eng.*, vol. 34, no. 2, pp. 170–180, Apr. 2009.

[43] M. A. Hossain, A. Karmaker, and M. S. Alam, "A low latency MAC protocol with reduced handshaking for provisioning spatial fairness in underwater sensor network," *Int. J. Wireless Inf. Netw.*, vol. 28, no. 2, pp. 147–161, Apr. 2021.

[44] H. H. Rizvi, S. A. Khan, R. N. Enam, K. Nisar, and M. R. Haque, "Analytical model for underwater wireless sensor network energy consumption reduction," *Comput., Mater. Continua*, vol. 72, no. 1, pp. 1611–1626, 2022.

[45] S. H. Bouk, S. H. Ahmed, and D. Kim, "Delay tolerance in underwater wireless communications: A routing perspective," *Mobile Inf. Syst.*, vol. 2016, pp. 1–9, Dec. 2016.

[46] R. Rachman, E. P. Laksana, D. S. Putra, and R. F. Sari, "Energy consumption at the node in underwater wireless sensor network (UWSNs)," in *Proc. 6th UKSim/AMSS Eur. Symp. Comput. Model. Simul.*, Malta, Malta, Nov. 2012, pp. 418–423.

[47] C.-C. Hsu, M.-S. Kuo, C.-F. Chou, and K. C.-J. Lin, "The elimination of spatial–temporal uncertainty in underwater sensor networks," *IEEE/ACM Trans. Netw.*, vol. 21, no. 4, pp. 1229–1242, Aug. 2013.
[48] N. Sun, X. Wang, G. Han, Y. Peng, and J. Jiang, "Collision-free and low delay MAC protocol based on multi-level quorum system in underwater wireless sensor networks," *Comput. Commun.*, vol. 173, pp. 56–69, May 2021.
[49] F. Bouabdallah, C. Zidi, R. Boutaba, and A. Mehaoua, "Collision avoidance energy efficient multi-channel MAC protocol for UnderWater acoustic sensor networks," *IEEE Trans. Mobile Comput.*, vol. 18, no. 10, pp. 2298–2314, Oct. 2019.
[50] F. A. Alfouzan, "Energy-efficient collision avoidance MAC protocols for underwater sensor networks: Survey and challenges," *J. Mar. Sci. Eng.*, vol. 9, no. 7, p. 741, Jul. 2021.
[51] E. M. Sozer, M. Stojanovic, and J. G. Proakis, "Underwater acoustic networks," *IEEE J. Ocean. Eng.*, vol. 25, no. 1, pp. 72–83, Jan. 2000.
[52] Z. Jin, M. Ding, Y. Luo, and S. Li, "Integrated time synchronization and multiple access protocol for underwater acoustic sensor networks," *IEEE Access*, vol. 7, pp. 101844–101854, 2019.
[53] Y. Chen, Z. Jin, Q. Zeng, and Q. Yang, "A collision-avoided MAC protocol with time synchronization and power control for underwater sensor networks," *IEEE Sensors J.*, vol. 22, no. 19, pp. 19073–19087, Oct. 2022.
[54] X. Su, S. Chan, and M. Bandai, "A cross-layer MAC protocol for underwater acoustic sensor networks," *IEEE Sensors J.*, vol. 16, no. 11, pp. 4083–4091, Jun. 2016.
[55] J. Jagannath, A. Saji, H. Kulhandjian, Y. Sun, E. Demirors, and T. Melodia, "A hybrid MAC protocol with channel-dependent optimized scheduling for clustered underwater acoustic sensor networks," in *Proc. 8th ACM Int. Conf. Underwater Netw. Syst.*, 2013, pp. 1–8.
[56] J. Liu, Z. Wang, M. Zuba, Z. Peng, J.-H. Cui, and S. Zhou, "DA-Sync: A Doppler-assisted time-synchronization scheme for mobile underwater sensor networks," *IEEE Trans. Mobile Comput.*, vol. 13, no. 3, pp. 582–595, Mar. 2014.
[57] G. Isbitiren and O. B. Akan, "Three-dimensional underwater target tracking with acoustic sensor networks," *IEEE Trans. Veh. Technol.*, vol. 60, no. 8, pp. 3897–3906, Oct. 2011.
[58] Z. Zhang, W. Shi, Q. Niu, Y. Guo, J. Wang, and H. Luo, "A load-based hybrid MAC protocol for underwater wireless sensor networks," *IEEE Access*, vol. 7, pp. 104542–104552, 2019.
[59] Y. Su, Y. Zhu, H. Mo, J. H. Cui, and Z. Jin, "UPC-MAC: A power control MAC protocol for underwater sensor networks," in *Proc. 8th Int. Conf.* Berlin, Germany: Springer, 2013, pp. 377–390.
[60] H. Wang, Y. Li, T. Chang, and S. Chang, "An effective scheduling algorithm for coverage control in underwater acoustic sensor network," *Sensors*, vol. 18, no. 8, p. 2512, Aug. 2018.
[61] S. Zhang, L. Qian, M. Liu, Z. Fan, and Q. Zhang, "A slotted-FAMA based MAC protocol for underwater wireless sensor networks with data train," *J. Signal Process. Syst.*, vol. 89, no. 1, pp. 3–12, Apr. 2016.
[62] A. A. Syed, W. Ye, and J. Heidemann, "Comparison and evaluation of the T-Lohi MAC for underwater acoustic sensor networks," *IEEE J. Sel. Areas Commun.*, vol. 26, no. 9, pp. 1731–1743, Nov. 2008.
[63] H. Y. Hwang and H.-S. Cho, "Throughput and delay analysis of an underwater CSMA/CA protocol with multi-RTS and multi-DATA receptions," *Int. J. Distrib. Sensor Netw.*, vol. 12, no. 5, May 2016, Art. no. 2086279.
[64] C.-M. Chao, M.-W. Lu, and Y.-C. Lin, "Energy-efficient multichannel MAC protocol design for bursty data traffic in underwater sensor networks," *IEEE J. Ocean. Eng.*, vol. 40, no. 2, pp. 269–276, Apr. 2015.

YE CHEN received the B.E. and M.E. degrees from the University of Electronic Science and Technology of China (UESTC), Chengdu, China. He is currently pursuing the Ph.D. degree with the School of Electrical and Information Engineering, Tianjin University, China. He is also a Lecturer with the School of Applied Science and Technology, Hainan University. His research interest includes underwater wireless sensor networks.

ZHIGANG JIN received the Ph.D. degree in electrical engineering from Tianjin University, Tianjin, China, in 1999. He was a Visiting Professor with Ottawa University, Ottawa, Canada, in 2002. He is currently a Professor with Tianjin University. His research interests include underwater sensor networks, social networks, and deep learning.

GUOZHEN XING was born in 2002. She is currently pursuing the B.E. degree in electronic science and technology with Hainan University, China. Her research interest includes underwater wireless sensor networks.

QINYI ZENG was born in 2001. She is currently pursuing the B.E. degree in electronic science and technology with Hainan University, China. Her research interest includes underwater wireless sensor networks.

YUEYAN CHEN was born in 2002. She is currently pursuing the B.E. degree in electronic science and technology with Hainan University, China. Her research interest includes underwater wireless sensor networks.

ZIYU ZHOU was born in 2002. He is currently pursuing the B.E. degree in electronic science and technology with Hainan University, China. His research interest includes underwater wireless sensor networks.

QIULING YANG received the B.E. degree from Shenyang Aerospace University, Shenyang, China, in 2003, the M.E. degree from Guangxi University, Nanning, China, in 2010, and the Ph.D. degree from Tianjin University, Tianjin, China, in 2016. She is currently a Professor and a Doctoral Supervisor with Hainan University, Haikou, China. Her research interests include protocol design and security of underwater acoustic sensor networks.